Investigation of the Effects of Nonlinear Model of Super-capacitors in Local DC Microgrids Supplied by Renewables

Conference Paper · September 2012

DOI: 10.1109/EPEPEMC.2012.6397331

CITATIONS
2

READS
166

3 authors, including:

Balázs Rakos
Budapest University of Technology and Economics
13 PUBLICATIONS **103** CITATIONS
SEE PROFILE

Peter Stumpf
Budapest University of Technology and Economics
58 PUBLICATIONS **224** CITATIONS
SEE PROFILE


EPE
pels
IEEE POWER ELECTRONICS SOCIETY
Powering a sustainable future
IEEE
EPE - PEMC
EAST
WEST
TECHNOLOGY BRIDGE
15th International Power Electronics and Motion Control Conference and Exposition
EPE-PEMC 2012 ECCE Europe
NOVI SAD, SERBIA
Organized by:
University of Novi Sad
Faculty of Technical Sciences
Novi Sad
EPE - PEMC
EAST
WEST
TECHNOLOGY BRIDGE
EPE PEMC
Supported by:
Provincial Secretariat for Science and Technological Development and High Education of AP Vojvodina
Ministry of Education, Science and Technological Development of Republic of Serbia
Sponsored by:
SIEMENS
DELTA
FROBAS
the electronic & chip experts
Typhoon HIL
September 4-6, 2012, Novi Sad, Serbia

Investigation of the Effects of Nonlinear Model of Super-capacitors in Local DC Microgrids Supplied by Renewables

Balázs Rakos[1], Péter Stumpf[1], István Nagy[1]

[1]Budapest University of Technology and Economics, Department of Automation and Applied Informatics
Budapest, Hungary, e-mail: rakos@get.bme.hu

***Abstract* — The first part of the paper offers an overview of the state-of-art of microgrids, their architectures and the control of AC microgrid. Its second part focuses on the dynamics of the DC microgrid control taking into account an ideal and a nonlinear model of supercapacitors. It compares the transient processes obtained by simulation by using the two different supercapacitor models.**

Keywords — Microgrid, distributed power generation, renewable energy, microgrid control, super-capacitor, energy storage.

I. INTRODUCTION

One of the greatest challenges of our civilization is to ensure continuous, reliable energy supply. The electric energy has certain priority. Its interruption even in a few seconds can cause serious damage for sensitive consumers and if it lasts longer it can create economic disaster. A developed country can be defeated by her enemy by laying down most of the electric energy sources. The availability of electric energy in high quality is vital both in short and in long run.

A paradigm shift is taking place in the electric energy production, transmission and distribution. One ingredient is the complete dependence of our daily life on electric energy. There are many others: the fossil fuel supply is gradually, slowly but surely getting depleted, the growing social resistance against the application of nuclear energy, the dangerous level of environment pollution, the warm house effect, the ever increasing demand for more energy especially in developing countries (China, India, Brazil, …) just to mention the main driving forces behind the paradigm shift. Fortunately our ability to cope with this new challenges has been enhanced dramatically due to the tremendous and spectacular advancements within the technology such as power electronics, material science including semiconductors, microelectronics, computers, communications, software technology, internet, etc. and their theoretical background.

All of these changes, developments forced us on the one hand and enabled us on the other hand to start utilizing in ever growing extent the renewable (wind, solar, biomass, …) and waste energies. Their availability in geographical term is disperse leading directly to the disperse, distributed electric energy production and to the paradigm shift in the electric energy generation, transmission and distribution. The clear, uniform structure consisting of the electric power production in central, large, sometimes giant power plants operating in three-phase, 50 or 60 Hz medium voltage, the more or less long or very long high voltage transmission line and the medium-low voltage distribution system changes in many senses into a mixed network. Due to the disperse renewable and waste energy sources distributed power generation (DPG) is spreading everywhere within the power system. In many cases transmission line is not needed as the DPG is right in the district of consumers. This way transmission loss is avoided, overall efficiency and reliability are increased. The generated power can be DC photovoltaic (PV) solar, variable frequency, variable voltage AC (wind) or even rather high frequency AC power (waste energy recovery, from pressure reduction in gas pipe line). The power level in DPG can change from kW to many MW. Without going into any further details, right at the first glance it can be seen that the new electric power system has many salient, distinct properties, substantially different from the traditional one creating many new challenges. The paper addresses only three of these challenges: 1) How the new architectures of the power system should or could look like on distributed level. 2) What kind of control issues emerge and how their solution can be in the new power architectures mainly in the microgrids. 3) How is the dynamics of DC microgrid influenced by the modeling of super-capacitor.

II. MICROGRID ARCHITECTURES

At the dawn of the DPG a few publications suggested the central control of the individual power sources both the small and medium size units similar to the traditional power systems. It would have led a very sophisticated and probably highly unreliable complex control network. Very soon a better concept, the microgrid solution replaced the idea of the overall central control.

Microgrid is a small, independent power system for increasing reliability with distributed generation, facilitating the integration of alternative renewable and waste energy recovery sources and enhancing efficiency by reduced transmission length. Wikipedia defines the microgrid as a localized grouping of electricity sources and loads that normally operates connected to and synchronous with the traditional centralized grid but can disconnect and function autonomously as physical and/or economic conditions dictate. Due to its ability to operate independently it reduces the impact of large scale blackouts, improves grid reliability and reduces dependence on transmission gird. Additional benefit is the opportunity to recapture heat that is often a wasted byproduct of electricity generation and it can be used to heat neighbouring buildings. This co-generation of heat and electricity is especially attractive helping to improve the economics and efficiency. The microgrid can be thought of as an individual controlled unit in the power

system which can have load and source as well.

Some of the microgrid features, most of them distinct ones are as follows: They have the ability to operate in islanded mode or connected to the utility grid. They must have DPG. Because of intermittency, fluctuation of renewable power sources (solar, wind, …), energy storage devices (battery, flywheel, supercapacitance, fuel-cell, superconducting coil, …) have to be incorporated together with fossil fuel based back up (e.g. gas, diesel engine, microturbine, …). They can have only AC or only DC bus or both. They are called microgrid with hybrid architecture. The microgrid can have a third bus with "high frequency" for special loads (lighting). All or most energy sources, loads and storages can be connected to the bus via power converters when required by bidirectional ones providing individual control. Interconnection, step up-down function and isolation can be done without heavy, bulky network transformer. Special and distinct protection strategy is needed as the active power flow can be bidirectional. Some authors think that even the application of thermo-mechanical switchgears can be avoided. Another feature of paramount importance in terms of economy in the new paradigm that microgrid can provide not only electric power but heat to its local area which otherwise would be wasted.

Turning to the architecture of microgrids, there are strong arguments and incentives for using both AC and DC microgrids [7]. Most of the conventional loads, appliances require 50/60 Hz supply. Many of small and medium size power sources are meeting this demand (UPS, diesel generators, stand-by supplies). On the other hand, some of the main renewable energy sources are generating DC power (solar and fuel cells) or their variable voltage and frequency is rectified anyway (wind mills, microturbines). Furthermore, storage devices are or can be DC sources (batteries, super-capacitors or flywheels, superconductive coils). On the load side many of them require DC power (consumer electronics, computers, analog-digital controllers, electronic gadgets, LED lighting, etc). On the top of it the DC-DC conversion technology is highly advanced especially in small and medium power level that it can meet most of the requirements within DC-DC frame economically with high efficiency.

AC microgrids have the benefit of using the well-developed AC grid technologies. On the other hand, contrary to the AC microgrids, the DC ones do not have a few drawbacks as follows: There is no need here for synchronization, reactive power compensation. Static and dynamic stability problems, skin effect, eddy current loss, voltage shape distortion, harmonics, subharmonics, unbalance, positive, negative and zero sequence components do not exist here in the sense we meet them in conventional large scale AC power systems.

Consequently both AC and DC microgrids are viable solutions, either separately or as an interconnected hybrid network. Both of them can work in islanded mode or grid connected. All three hierarchical configurations are technically feasible (Fig.1). Either the AC or the DC microgrids can be located on level 1 or on level 2. In the third configuration both the AC and the DC microgrids are interfacing the utility grid and they are interconnected to each other in order to back-up one by the other in islanded mode or when one of the utility grid connection fails. Between the utility grid and the AC microgrid controlled P and Q power flow take place while the DC microgrid can accept only active power but both P and Q power can be drawn from it.

Synchronization is needed when the AC microgrid has to be connected to the utility grid. Returning from islanded mode to grid connected operation is simpler for DC microgrids. When the load power or the power of the renewable energy sources connected to the DC microgrid is significantly higher than those connected to the AC microgrid direct interconnection of the DC microgrid to the utility grid makes sense. Consider a DC microgrid recharging large number of electric vehicles or a solar power plant of high power supplying most of its power to the utility grid. In these cases the second architecture with AC microgrid on Level 1 and DC microgrid on Level 2 is a more economical arrangement. The argument for the order of the microgrids applies in reverse direction. Currently the AC load in the distribution network mostly surpasses the DC one, and therefore the DC-AC-utility architecture is expected to be applied mostly. More sophisticated architectures of microgrids are viable in order to increase the reliability. There can be two or more microgrids on the same level interconnected to each other but can work in islanded mode as well.

The exponential increase in the number of publications on microgrids shows that the concept is rather new, 10 years back papers could be scarcely found on the topic. The expectation of its wide-spread application is high. There are other classifications beside AC and DC microgrids. Experts talk about residential, industrial, military, remote microgrids or the one supplying sensitive loads.

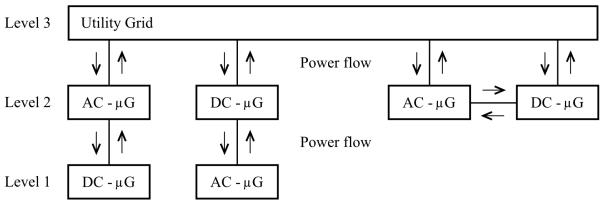

Fig. 1. Hierarchical configurations of microrids (μG)

The theoretical and experimental research has been going on world-wide. Pike Research reported on May 24, 2011 that more than 160 microgrid projects are currently active around the world [3].

Few authors do not make difference between the term Smart Grid and microgrid. Smart Grid is introduced rather recently for digitally enabled electrical grid that collects and dispatches data and acts on them to improve operation, stability reliability, efficiency, economics, … Other definitions can be found using other words with similar meaning. Its hardware components are embedded processors, smart meters, sensors and its softwares are SCADA, Energy management, etc. Smart Grid is a more general term than microgrid, the whole modern electric network can be a Smart Grid while the microgrid is only a small fraction of the whole network or it can be totally independent (remote microgrid).

The microgrid research has taken a somewhat different direction in the USA than the target was in Europe and Japan [4,5]. The reason is that the reliability of electric power service is poorer in the USA. The demand from the

microgrid is to seamlessly island during utility fault and again seamlessly reconnect when the normal service reestablished. In other words they should work like an uninterruptable power supply. Otherwise all other main incentives are the same. One of the well-known researches is the CERTS (Consortium for Electric Reliability Solutions) microgrid program with numerous participants. Another research program is led by the General Electric Global Research. Both of them are co-funded by the US Department of Energy (DOE). Likely significant global impact will be resulted in the IEEE standard process developing of IEEE P1547.4 Draft Guide for Design, Operation and Integration of Distributed Island Systems with Electric Power Systems. Turning to Europe research was funded by EUR 7.85 Million within the European Union in the frame of FPG project "More Microgrids". Three microgrid field tests have been started as early as 2005 in Japan. Their power was 710, 750 and 2400 kW, respectively [1]. Another paper reported 5 microgrid related projects from Japan, they are: Hachinoche, Sendai, Akayi, Aichi and Kyoto projects [2].

III. AC MIRCOGRID CONTROL

Simple model of the AC microgrid seleted for the study of its control is shown in Fig. 2. The voltage source converter (VSC) plus the DC source block represent the general model of the microsources, the distributed generation (DG) units. Most of the sources provide DC power, such as fuel cells, solar cells, battery and super-capacitor storages or the microturbines generating high frequency AC which has to be rectified. The DC power can come from the DC microgrid as well through bidirectional converter. All of them are connected to the AC microgrid via VSC. The AC load block represents the load. The VSC is coupled to the AC microgrid through transformer or chock represented by reactance X at the point of common coupling (PCC) which is connected to the utility grid by switch S. If a synchronous generator or compensator is part of the AC microgrid they are modeled basically in similar way by an internal voltage $\boldsymbol{V_o}$ and a series (synchronous) reactance. The DG units can apply either the conventional current controlled VSC (CC-VSC) or the voltage controlled VSC (VG-VSC). The second strategy is used in the current paper.

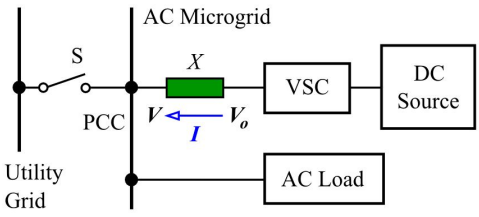

Fig. 2. Simple model of AC microgrid

In grid connected mode switch S is on and both the frequency and the voltage $\boldsymbol{V}$ are dictated by the utility grid [5]. The voltage space vector of the utility grid $\boldsymbol{V}$ and that of the VSC output voltage $\boldsymbol{V_o}$ together with reactance X determine the P active and Q reactive power flow between the two grids by (1) and (2):

$$P = \frac{3}{2}\frac{VV_0}{X}\sin\vartheta \tag{1}$$

$$Q = \frac{3}{2}\frac{V}{X}(V - V_0\cos\vartheta) \tag{2}$$

where V and V_0 are peak values and ϑ is the angle between $\boldsymbol{V}$ and $\boldsymbol{V_0}$.

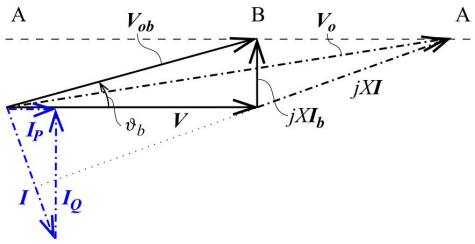

Fig. 3. Voltage space vector diagram

Fig. 3 shows the voltage space vector diagram in grid connected mode at a border case when only active power exchange takes place between the two grids, the reactive power Q is zero; $V = V_{0b}\cos\vartheta$.

Assuming, that P and V are kept constant that is the $\boldsymbol{I}_p$ active component of $\boldsymbol{I}$ is constant and V_0 is increased or decreased, the peak point of $\boldsymbol{V}_0$ and $jX\boldsymbol{I}$ are moving along dotted line *A-A*. Inductive or capatitive current component $\boldsymbol{I}_Q$ and reactive power flow Q can be set by V_0. On the other hand, keeping the absolute value of $\boldsymbol{V}$ and $\boldsymbol{V}_0$ constant and changing only the active power P, angle ϑ varies and the reactive power change is $\Delta Q = tg\vartheta\Delta P$. When ϑ is small the reactive power change can be negligible. The power P and Q can be changed independently upon each other. P is controlled by ϑ, Q is controlled by V_0.

In islanded mode the distribution of reactive and active power among the sources and loads, the stable operation of the microgrid have to be taken care of. Now neither the voltage V nor the frequency is forced on the microgrid they can be changed.

Voltage regulation by voltage droop [5,6,8]. Two or more ideal voltage sources cannot be connected to the same grid, they cannot work in parallel in stable way, large circulating reactive current can develop. In principle, the simplest solution is the same applied in bus bars in power plants fed from synchronous generators. The grid voltage V is kept constant in our case by changing the output voltage of the inverter V_0 as a function of the reactive power Q (or reactive current I_Q) in the fashion given by (3).

$$V_0' = V + K_V Q \tag{3}$$

when I is laging V then $V_0' > V$. Conversely in the capacitive regiven $V_0' \square V$ (Fig.4). V_0' is approximately the absolute value of the space vector $\boldsymbol{V}_0'$ behing $\boldsymbol{V}$. The reactance between them is X' which can be smaller,

equal or higher then X depending in the voltage drop constant K_V. By selecting K_V in appropriate way, the reactive power can be shared in the ratio of rated power among the units connected to the microgrid. The maximum reactive power of a unit $Q_{max} = S_{rated} - P_{rated}$ where S and P are the apparent and active power.

The voltage regulation is realized by the block diagram shown in Fig. 5. V^* and V is the reference and grid measured value of the microgrid voltage, respectively. Q is the measured value of the reactive power of the respective DG Unit. $Q > 0$ in inductive reactive power. *PI* is the voltage controller.

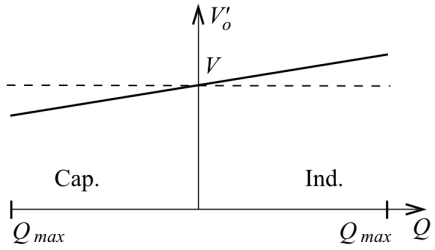

Fig. 4. Voltage droop as a function of Q

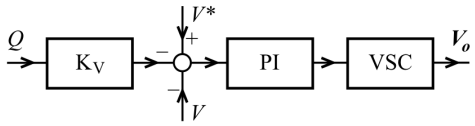

Fig. 5. Voltage regulation

Power sharing by frequency droop [6,8]. The power-frequency controller of the DG units takes care of autonomous power tracking in load variation and power sharing among the DG units connected to the microgrid in islanded mode. The frequency f of each of the DG units in islanded mode in steady-state is given by (4).

$$f = (P^* - P)K_f + f_0 \tag{4}$$

where f_0 is the base frequency, P^* is the reference power, P is the power of the microsource (DG unit), K_f is the frequency droop constant.

Assume that the microgrid has three microsources; DG_a, DG_b and S (Fig.6). The first two are generating power, S is energy storage unit. First the microgrid is connected to the utility grid importing active power and $f = f_0$. The operation points are: 1, 2 and 3. The power supplied by DG's is proportional to their respective reference power. The energy storage unit is charging. Its operation point is 3. Due to blackout or fault the network connection is lost, the microgrid is switched into islanded mode. To ensure the power balance the frequency drops f_u or f_l. The power generated by DG_a and DG_b is increased to supply the load and changing the storage unit S. The new operation points when $f = f_u$ are 4, 5 and 6 (Fig. 6). If the power demand of the load is getting higher the frequency is further reduced to f_l establishing operation points 7,8 and 9. Now the storage unit is discharging, The microsources generate their rated or maximum power at frequency $f = f_{\min}$.

In case of exporting power to the utility grid by the microgrid before switching into islanded mode the frequency increases and the generated power by the microsources is reduced; the storage unit gets charged by higher power.

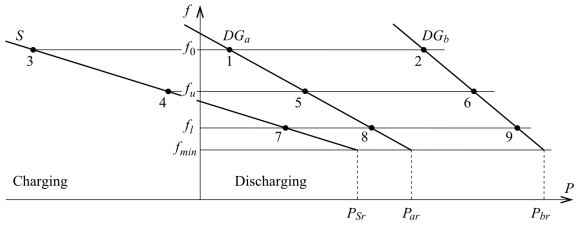

Fig. 6. Power balance by frequency droop

The order of magnitude for $K_f = \Delta f / \Delta P = 0.5Hz / 1pu$ power error applied for DG units and $K_f = 0.5Hz$ droop for 1.5 *pu* power error in case of energy storage as it works both in charging and discharging mode.

In the dynamics in frequency change the angle between the space vector $\boldsymbol{V}$ and $\boldsymbol{V}_0$ is changing together with the generated power. Gradually the two vectors are reaching their final frequency in each microsources.

IV. DC Microgrid Control and its Dynamics

The configuration of the DC microgrid considered in the current paper is shown in Fig.7. It has a high voltage (e.g. 400 V) bus for higher power loads and a low voltage (e.g. 24 V) bus for the low power loads. They are interfaced by a DC-DC converter. The renewable sources are represented by one block and connected through a DC-DC converter to the high voltage bus. The application of only two storage devices, the battery and the super-capacitor is assumed. An AC-DC bidirectional converter connects the V high DC bus to the AC grid which can be either the AC microgrid or the utility grid. As further power source rotating generators via AC-DC converter supplies power to the V high DC bus. The loads can be interfaced to the bus through converters for voltage matching. For simplicity and for our study they are ignored.

All of the converters are controlled. The DC-DC converter between the two buses controls the voltage of the low voltage DC bus.

Similarly the AC-DC converter connecting the rotating generators to the DC bus is responsible for voltage control of the V_{high} DC bus by its VC voltage controller. The reference values of the controllers are denoted by letters with star, e.g. i_S^*.

During the simulations below we focus on the impact of the super-capacitor models on the dynamic processes of the microgrid.

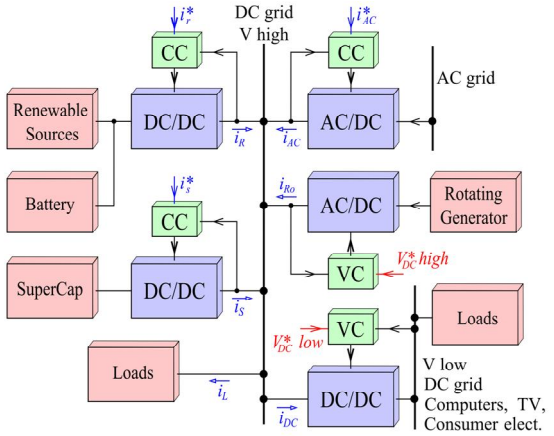

Fig. 7.Configuration of DC Microgrid

Modeling of super-capacitor. The operation of super-capacitors (SC) or electric double-layer capacitors (EDLC) is based on electrochemical processes. The SC model applied by [10-12] can be characterized by

$$Z(j\omega) = R + \frac{1}{Cj\omega}. \qquad (5)$$

A real, commercially available SC, however, deviates from this behavior. Several different models can be found in the literature providing more accurate descriptions [13 -20]. The model based on [16] is becoming insufficient above around 400 mHz [21] due to the non-integer order behavior of the SC characteristic.

Our simulations will be based on the model of [18], since it gave a better description of the SC characteristics than other models when compared to experimental results [21]. Few parameters are sufficient. The model is

$$Z(j\omega) = R + \frac{\left(1+\frac{j\omega}{\omega_0}\right)^{\alpha}}{C(j\omega)^{\beta}}, \qquad (6)$$

where C is the capacitance, R is the series resistance of SC, α, β, and ω_0 are parameters that can be determined experimentally.

The parameters are provided in TABLE I by [24] in the case of a commercially available SC (BPAK0058-15V, C=58 F, R=0.019 Ω, Maxwell Technologies). We will use these data during simulations.

The comparison of the models characterized by (5) and (6) in the case of the parameters provided by TABLE I and the manufacturer are displayed in Fig. 8 with normal (black) and dotted (blue) lines, respectively. Significant difference can be detected between the results using (5) and (6) even in very low (Fig.8a) and in higher (Fig.8b) frequency ranges.

TABLE I
MODEL PARAMETERS OF THE SUPER-CAPACITOR DETERMINED BY [24]

Operating point	1 V	9V
α	0.813	0.579
β	0.99	0.989
R_S	0.0204 Ω	0.0208 Ω
C	42.36 F	55.3 F
ω_0	2.07 rad/s	0.994 rad/s

In order to provide a formula that can be applied easier than (6) during simulations, we performed the Taylor series expansion of $\left(1+\frac{j\omega}{\omega_0}\right)^{\alpha}$ to the third order around $j\omega = 0$:

$$\left(1+\frac{j\omega}{\omega_0}\right)^{\alpha} \approx 1+\frac{\alpha j\omega}{\omega_0}+\frac{(\alpha^2-\alpha)(j\omega)^2}{2\omega_0^2}+ \\ +\frac{(\alpha^3-3\alpha^2+2\alpha)(j\omega)^2}{6\omega_0^3}. \qquad (7)$$

Furthermore, we assumed $\beta = 1$, since it is almost unity (TABLE I).

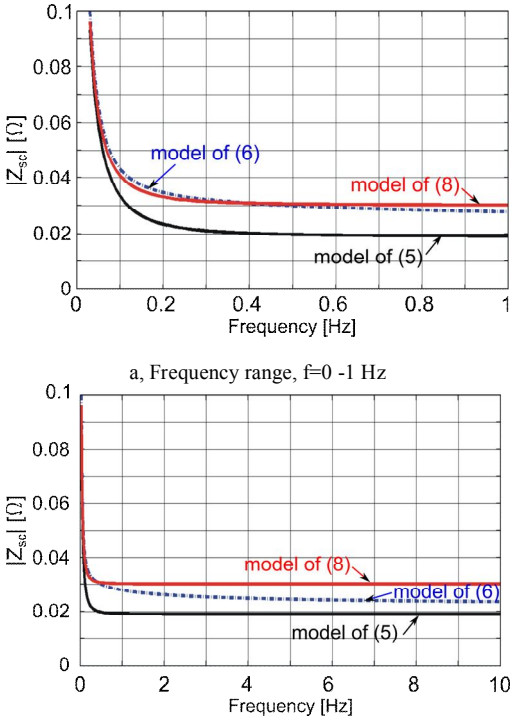

a, Frequency range, f=0 -1 Hz

b, Frequency range, f=0 - 10 Hz

Fig. 8.Magnitude of the impedance of SC as the function of frequency according to the models described by (5),(6) and (8) at 9V

The simplified impedance expression with the first order Taylor expansion approximates of (6) will be used in the simulation.

$$Z(j\omega) = R + \frac{\alpha}{C\omega_0} + \frac{1}{Cj\omega}, \qquad (8)$$

therefore a simple circuit model consisting of a voltage-dependent resistance $R' = R + \frac{\alpha}{C\omega_0}$ in series with a voltage-dependent capacitor C can approximate. The voltage dependence originates from TABLE I as C and ω_0 depend on voltage v_{sc}.

In the following we will assume that α and ω_0 also have a linear dependence on the voltage. In the case of α:

$$\alpha = \alpha_0 + K_\alpha v_{SC}, \qquad (9)$$

where $\alpha_0 = 0.842$ and $K_\alpha = -0.029\text{V}^{-1}$. In the case of ω_0:

$$\omega_0 = \omega_{00} + K_{\omega_0} v_{SC}, \qquad (10)$$

where ω_{00} = 2.205rad/s and $K_{\omega 0}$ = -0.135rad/Vs. Since R has a moderate dependence on the voltage (see TABLE I), we assume that it has a value of R = 0.02Ω independent of the voltage.

The voltage dependence of C can be characterized by a linear equation according to [24]:

$$C = C_0 + K_C v_{SC}, \tag{11}$$

where C_0 = 44.2F and K_C = 1.53F/V.

The comparison between (6) and (8) are displayed in Fig.8. In the case of the very low frequency range practically there is no difference (see Fig.8a).

V. Simulation Results

The block diagram of the DC Microgrid shown in Fig.7 was implemented in Matlab/Simulink environment by using the SimPowerSystem toolbox to study the dynamic current sharing of the system in the time domain by using ideal and nonlinear SC models. For simplicity the bidirectional DC/DC converters, presented in more details in [12], are modeled by using their average-value model. Furthermore, it was assumed that the microgrid is not connected to the AC grid and the renewable sources connected to the battery do not produce any electric energy. Thus, only the battery, the super-capacitor and the rotating generator supply the load. For simplicity the rated DC link voltage of the simulated microgrid is V_{DC}=24 V.

The implemented Simulink model of the SC based on (8) is displayed in Fig.9. During the simulation study this model is compared to an ideal capacitor connected in series with a constant resistance (C=58 F, R=0.019 Ω, from datasheet).

The reference current of the SC is controlled by the load current through a simple high pass filter and a one-energy storage element:

$$i_S^* = \left(\frac{\tau_1 s}{\tau_1 s + 1} + K_S \frac{1}{\tau_2 s + 1} \right) i_L \tag{12}$$

where K_S is the current sharing ratio for the SC. The reference signal for the current control loop of the battery is

$$i_R^* = K_B \frac{1}{\tau_2 s + 1} i_L \tag{13}$$

where K_B is the current sharing ratio for the battery. If K_S +K_B < 1, than the rotating generator ensures the remaining load current portion. The value of Ks depends on voltage v_{sc}, which is controlled by the V_{sc} slow voltage controller neglected in the paper.

First K_S = 0 and K_B = 0.5 are assumed. Thus, the super-capacitor handles only the large transients of the loading current and in steady-state its current is zero.

Fig.10 shows the time functions of i_s, i_R and i_{Ro}, when the load current changes stepwise from i_L=0.5 A to i_L=5A and nonlinear SC model is used. The initial voltage of the SC is V_{sc0} = 9 V. It can be observed that the SC handles the rapid transient, but in steady state the battery and the rotating generator equally shares the loading current while i_s = 0.

By using an ideal capacitor instead of the nonlinear SC model, the results for the currents versus time are practically the same as in Fig.10a due to the high performance of the relevant current and voltage control loops. The two $v_{sc}(t)$ functions, however, differ significantly due to the differences of the two models (Fig.10b).

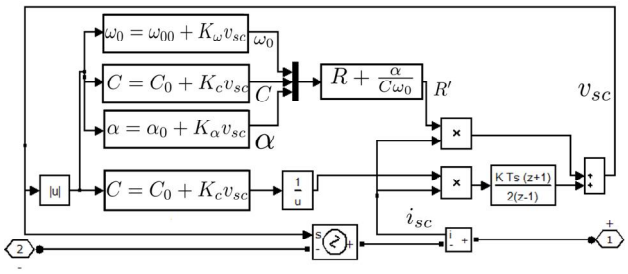

Fig. 9. Nonlinear super-capacitor model in Simulink by using SimPowerSystem toolbox

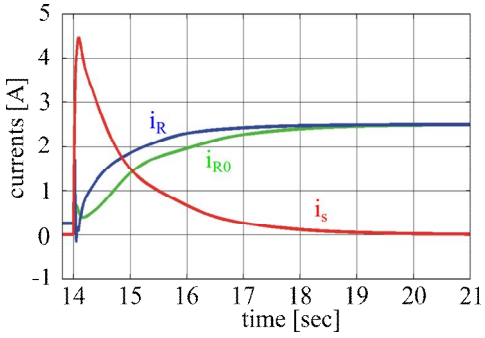

a, Time dependence of i_s, i_R and i_{Ro}, V_{sc0} = 9 V, nonideal supercap model

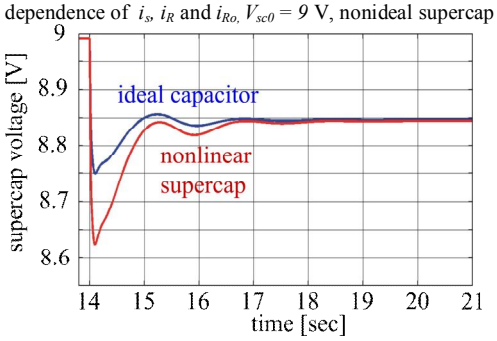

b, Time function of super-capacitor voltage, V_{sc0} = 9 V

Fig. 10. Sudden change in loading current, Δi_L=4.5A, K_S = 0 and K_B = 0.5

Figure 11 shows the time functions of the i_s current and the SC voltage, when two SCs are connected in series with identical initial voltage V_{sc0} = 4.5 V and the load current changes stepwise again from i_L=0.5A to i_L=5A. Based on (8) - (11) the capacitance and the resistance of the SC around 4.5V is $C \approx 51.1$ F and R = 0.0287 Ω. Again significant difference can be observed between the two $v_{sc}(t)$ curves while the $i_s(t)$ functions are practically the same.

Second K_S = 0.33 and K_B = 0.33 are assumed. Thus, the SC does not only handle the large transients, but supply the load in steady-state, as well. Fig.12 shows i_s, i_R and i_{Ro}, versus time when the load current changes stepwise again from i_L=0.5A to i_L=5A and V_{sc0} = 9V.

No difference is visible in the current waves, however, the $v_{sc}(t)$ functions differ from each other (Fig.12b). As the voltage decreases the capacitance of the SC decreases, as well and the slope of the discharge increases. It can be more clearly observed in Fig.12c, when two SCs are

connected in series with initial voltages V_{sc0} = 4.5 V for each.

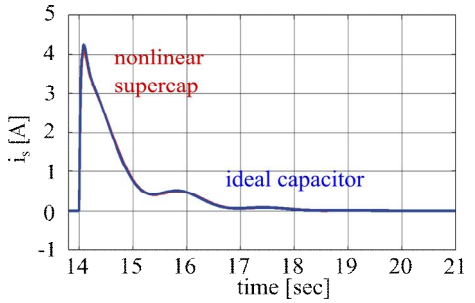

a, Time function of super-capacitor current, V_{sc0}=4.5V

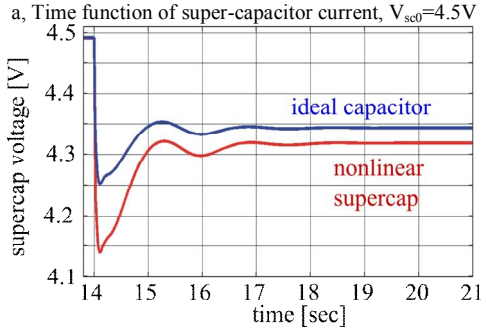

b, capacitor voltage, V_{sc0}=4.5V

Fig. 11. Sudden change in loading current, Δi_L=4.5A, K_S=0 and K_B = 0.5

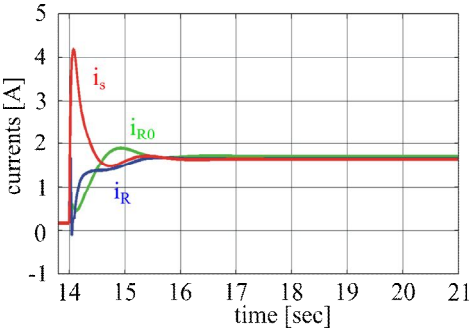

a, time dependence of i_s, i_R and i_{Ro}, V_{sc0} = 9 V, non-ideal SC model

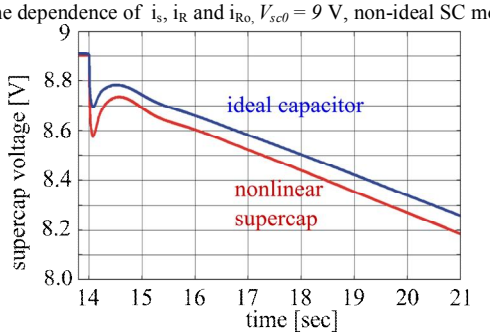

b, capacitor voltage, V_{sc0}=9V

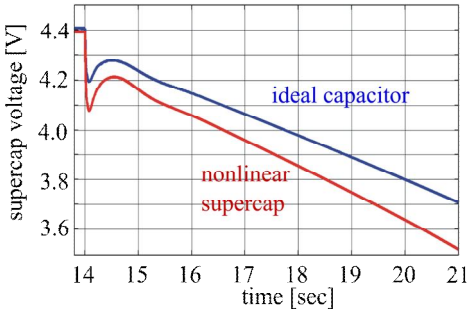

c, capacitor voltage, V_{sc0}=4.5V

Fig. 12. Sudden change in loading current, Δi_L=4.5A, K_S=0.33, K_B=0.33

VI. Conclusions

The first part of the paper shortly described the paradigm change in the electric energy production, transmission and distribution focusing in the concept of microgrid. After summarizing the architecture of microgrid and the control of AC microgrid it dealt in depth with the voltage control of DC microgrid. The DC microgrid structure treated in the paper included renewable and rotating generator sources, it had energy storage units, loads and connection for power transfer to AC grid. It investigated the voltage transient of the DC bus caused by a sudden change in the load current. It determined the time function of various variables for two supercapacitor models, first the model was a simple RC circuit, while in the second case it was a rather sophisticated nonlinear block describing the real supercapacitor quite accurately. As it was expected substantial difference can be observed only in the time function of the supercapacitor voltage and consequently in its energy stored by the supercapacitor. The study accentuate that the application of the simple RC model can be very misleading and in engineering design its not recommended.

Acknowledgement

The authors wish to thank the Hungarian Research Fund (OTKA K72338 and K100275) and the Control Research Group of the Hungarian Academy of Sciences (HAS). This work is connected to the scientific program of the "Development of quality-oriented and harmonized R+D+I strategy and functional model at BME" project. This project is supported by the New Széchenyi Plan (Project ID: TÁMOP-4.2.1/B-09/1/KMR-2010-0002)

References

[1] Funabashi T. „Microgrid fields tests experiences in Japan" Power Engineering Society General Meeting, IEEE, 2006.

[2] Morozumi S. "Overview of Micro-grid Research and Development Activities in Japan" symposium on Microgrids, Montreal June 23, 2006.

[3] http://www.pikeresearch.com

[4] Chris Marnay and Nan Zhou „Microgrid Research Activities in the US." Ernest Orlando Lawrence Berkely National Laboratory, February, 2008. http://eetd.gov/EA/EMP/

[5] Erickson, M.J. and Lasseter, R.H.:"Integration of Battery Energy Storage Element in a CERTS Microgrid", Energy Conversion Congress and Exposition, 2010, pp.2570-2577

[6] R.H. Lasseter: "Microgrids" in Proc. IEEE Power Eng. Winter Meeting, New York, Jan 2002

[7] Boroyevich, D. and Cvetkovic, I.:"Future Electronic Power Distribution Systems – A contemplative view", Optimization of Electrical and Electronic Equipment (OPTIM), 2010, 12th International Conference, pp.1369-1380

[8] G. Fang and M.R. Iravani: "A Control Strategy for a Distributed Generation Unit in Grid-Connected and Autonomous Modes of Operation", Power Delivery, IEEE Transactions, 2008, vol.23, pp.850-859

[9] S. Chopra, P. Bauer: "Driving Range Extension of EV with On-road Contactless Power Transfer – A Case study", IEEE Transactions on Industrial Electronics, 2012, ISSN: 0278-0046, early access on IEEEXplore

[10] A. Govindaraj, M. King, S.M. Lukic „Performance Characterization and Optimization of Various Circuit Topologies to Combine Batteries and Ultra-Capacitors", IEEE, IECON'10, 2010, USA, pp. 1844-1850.

[11] J.J. Awerbuch, Ch.R. Sullivan: „Control of Ultracapacitor-Battery Hybrid Power Source for Vehicular Applications", IEEE Energy 2030, Atlanta, USA, 17-18 Nov. 2008.

[12] B. Rakos, P. Stumpf, and I. Nagy, “Energy from Biogas, Renewables for Supplying Telecommunications in Remote, Rural Areas,” *2011 IEEE 33rd International Telecommunications Energy Conference (INTELEC)*.
[13] L. Zubieta, R. Bonet, “Characterization of Double-Layer Capacitors for Power Electronic Applications”, IEEE Trans. On Ind. Appl., vol. 36, no. 1, January/February 2000, pp. 199–205.
[14] S. Buller, E. Karden, D. Kok, R. W. De Doncker, ”Modeling of the Dynamic Behavior of Supercapacitors Using Impedance Spectroscopy”, IEEE Trans. On Ind. Appl., vol. 38, no. 6, November/December 2002, pp. 1622–1626.
[15] R. Kötz, M. Carlen, “Principles and Application of electrochemical capacitors”, Electrochimica Acta 45, 2000, pp. 2483–2498.
[16] A. Parreño, P. L. Roncero, V. Feliu, F. Castillo, “Fractional Dynamics Analysis of an Ultracapacitor Based Buck-Boost Power Electronic Converter”, 3rd Workshop of the International Federation of Automatic Control on Fractional Differentiation and its Applications FDA’08, Ankara, Turkey, November 2008.
[17] P. Mahon, G. L. Paul, S. M. Keshishian, A. M. Vasallo, “Measurement and Modelling of the High-Power Performance of Carbon-Based Supercapacitors”, Journal of Power Sources, no. 91, 2000, pp. 68–76.
[18] J. J. Quintana, A. Ramos, I. Nuez, “Identification of the Fractional Impedance of Ultracapacitors”, Proceedings of the 2nd IFAC Workshop on Fractional Differentiation and its Applications, Porto, Portugal, July 19–21, 2006.
[19] N. Bertrand, J. Sabatier, O. Briat, J. M. Vinassa, ”An Ultracapacitor Non-Linear Fractional Model”, 3rd Workshop of the International Federation of Automatic Control on Fractional Differentiation and its Applications FDA’08, Ankara, Turkey, November 2008.
[20] F. Rafik, H. Gualous, R. Gallay, A. Crausaz, A. Berthon, “Frequency, Thermal and Voltage Supercapacitor Characterization and Modelling”, Journal of Power Sources, no. 165, 2007, pp. 928–934.
[21] Farkas I., Vajk I., “Internal Model-based Controller for Solar Plant Operation”, Computers and Electronics in Agriculture, Vol. 49, Nr. 3, 2005, pp. 407–418.
[22] Vajk I., Hetthéssy J., “Load Forecasting using Nonlinear Modelling”, Control Engineering Practice, Vol. 13, Nr. 7, 2005, pp. 895-902.
[23] R. Martin, J. J. Quintana, A. Ramos, I. Nuez “Modeling Electrochemical Double Layer Capacitor, from Classical to Fractional Impedance”, Electrotechnical Conference, 2008. MELECON 2008. The 14th IEEE Mediterranean, pp. 61 - 66.
[24] M.F. Mathias, O. Haas, J. Phys. Chem. 97, 1993, pp..9217.
[25] H. Scher, M. Lax, Phys. Rev. B 7, 1973, pp. 4491.
[26] X. del Toro Garcia, P. Roncero-Sánchez, A. Parreno, V. Feliu, “Ultracapacitor-based Storgae: Modelling, Power Conversion and Energy Considerations”, Industrial Electronics (ISIE), 2010 IEEE International Symposium, pp. 2493 – 2498.
[27] F. van der Pijl, M. Castillia, P. Bauer, „Adaptive Sliding Mode Control for a Multiple-user Inductive Power Transfer System without need for Communication“, IEEE Transactions on Industrial Electronics, 2012, ISSN:0278-0046, early access on IEEEXplore
[28] F. Baalbergen, P. Bauer, “Power Management Strategies for Generator-Set with Energy Storage for 4Q load, IEEE Transaction on Industrial Electronics, May 2009, Vol. 56, Issue 5, pp.1485-1498, ISSN:0278-0046
[29] V. Moreno-Font, A. El Aroudi, J. Calvente, R. Giral, L. Benadero, „Dynamics and Stability Issues of a Single-Inductor Dual-Switching DC-DC Converter” IEEE Transactions on Circuits and Systems-I: Regular Papers, Vol 57, No. 2, February 2010, pp.415-426
[30] Kolokolov Y, Ustinov P, Essounbouli N, Hamaoui A, „Bifurcation-free design method of pulse energy converter controllers”, Chaos Solitons and Fractals, Vol.42, No.5, 2009, pp. 2635-2644
[31] El Aroudi A, Angulo F, Olivar G, Robert BGM, Feki M, „Stabilizing a two-cell DC-DC Buck Converter by Fixed Point Induced Control” International Journal of Bifurcation and Chaos, Vol. 19, Issue 6, 2009, pp. 2043-2057
[32] Ruscin, M. Lacko, M. Olejar, J.Dudrik, “Soft Switching PS-PWM DC-DC Converter Controlled by Microprocessors”, EDPE’07, High Tatras, Slovakia, 24 -26 Sept, 2007, CD rom ISBN: 978-80-8073-868-6
[33] V. Oleschuk, F. Profumo, A. Tenconi. „Simplifying Approach for Analysis of Space-Vector PWM for Three-Phase and Multiphase Converters” EPE’07, Aalborg, Denmark, 2-5 szept, 2007, CD Rom ISBN: 9789075815108
[34] D. Giaouris, S. Banerjee, B. Zahawi, V. Pickert, „Stability Analysis of the Continuous-Conduction-Mode Buck Converter Via Filippov’s Method” Circuits and Systems I. Regular Papers, IEEE Transactions on (Circuits an Systems I: Fundamental Theory and Applications, IEEE Transactions on, 2008, Vol 55, Issue 4, pp. 1084-1096
[35] Komrska, T., Žák, J., Ovaska, S., Peroutka, Z.: Computationally efficient current reference generator for 50-Hz and 16.7-Hz shunt active power filters. International Journal of Electronics. Vol. 97, No. 1, 2010, pp. 63 – 81. ISSN: 0020-7217. Taylor & Francis.
[36] Vajk I., “Identification Methods in a Unified Framework”, Automatica, Vol.41, Nr.8, 2005, pp.1385-1393